Chinese Chemical Letters 36 (2025) 109853

Contents lists available at ScienceDirect

Chinese Chemical Letters

journal homepage: www.elsevier.com/locate/cclet

Eco-friendly aqueous binder derived from waste ramie for high-performance Li-S battery

Shuang Ma[a,b,1], Guangying Wan[c,1], Zhuoying Yan[c], Xuecheng Liu[a,*], Tiezhu Chen[b], Xinmin Wang[a], Jinhang Dai[a], Juan Lin[b], Tiefeng Liu[c,d,e,*], Xingxing Gu[a,*]

[a] Chongqing Key Laboratory of Catalysis and New Environmental Materials, College of Environment and Resources, Chongqing Technology and Business University, Chongqing 400067, China
[b] Sichuan Provincial Key Laboratory of Quality and Innovation Research of Chinese Materia Medica, Sichuan Academy of Chinese Medicine Sciences, Chengdu 610041, China
[c] College of Chemical and Biological Engineering, Zhejiang University, Hangzhou 310027, China
[d] College of Materials Science and Engineering, Zhejiang University of Technology, Hangzhou 310014, China
[e] Quzhou Institute of Power Battery and Grid Energy Storage, Quzhou 324000, China

ARTICLE INFO

Article history:
Received 28 February 2024
Revised 8 March 2024
Accepted 1 April 2024
Available online 2 April 2024

Keywords:
Li-S battery
Ramie gum
Eco-friendly
Sulfur cathode
Polysulfides

ABSTRACT

Even the sulfur cathode in lithium-sulfur (Li-S) battery has the advantages of high theoretical energy density, wide source of raw materials, no pollution to the environment, and so on. It still suffers the sore points of easy electrode collapse due to large volume expansion during charge and discharge and low active materials utilization caused by the severe shuttle effect of lithium polysulfides (LiPSs). Therefore, in this work, ramie gum (RG) was extracted from ramie fiber degumming liquid and used as the functional binder to address the above problems and improve the Li-S battery's performance for the first time. Surprisingly, the sulfur cathode using RG binder illustrates a high initial capacity of 1152.2 mAh/g, and a reversible capacity of 644.6 mAh/g after 500 cycles at 0.5 C, far better than the sulfur cathode using polyvinylidene fluoride (PVDF) and sodium carboxymethyl cellulose (CMC) binder. More importantly, even if the active materials loading increased to as high as 4.30 mg/cm^2, the area capacity is still around 3.1 mAh/cm^2 after 200 cycles. Such excellent performances could be attributed to the abundant oxygen- and nitrogen-containing functional groups of RG that can effectively inhibit the shuttle effect of LiPSs, as well as the excellent viscosity and mechanical properties that can maintain electrode integrity during long-term charging/discharging. This work verifies the feasibility of RG as an eco-friendly and high-performance Li-S battery binder and provides a new idea for the utilization of agricultural biomass resources.

Sulfur as the cathode material of Li-S battery, owns a theoretical energy density of up to 2600 Wh/kg, and sulfur cathode material has rich resources, low cost, environment friendly, *etc.* [1,2]. Nonetheless, Li-S battery still faces some serious problems, such as poor conductivity of active substances, severe shuttle effect caused by the intermediate Li Polysulfides (LiPSs) dissolved into electrolytes, and the volume expansion of sulfur electrodes during cycling. In order to solve the above problems of Li-S batteries, considerable efforts include the structural design of S-based cathode materials [3,4], chemical optimization of liquid [5], and the development of new functional binders and separators [6], in addition, the problem of anode dendrite growth has also been widely studied [7–9]. Among them, the binder is a small part of the sulfur cathode, and its important functions are often neglected. In recent years, its important functions have gradually emerged [10]. This is because in addition to its inherent "glue" effect, the binder can also rely on polar functional groups to limit the shuttle of LiPSs and provide good mechanical properties to alleviate the volume expansion of the sulfur cathode, thereby increasing the utilization of sulfur active substances.

Traditional commercial binders, such as PVDF binder, have serious environmental and health problems because it is an unsustainable oil-based material and needs to be dissolved into toxic *N*-methyl pyrrolidone (NMP). Another common commercial binder CMC, although dissolves in aqueous solvent, it still has the draw-

* Corresponding authors.
E-mail addresses: liuxc@ctbu.edu.cn (X. Liu), tiefengliu@zju.edu.cn (T. Liu), x.gu@ctbu.edu.cn (X. Gu).
[1] These authors contributed equally to this work.

https://doi.org/10.1016/j.cclet.2024.109853
1001-8417/

backs of poor mechanical stability, as well as lacks enough LiPSs fixation sites [11], as a result, active substances are easy to lose in the process of volume change, and hardly improving the sulfur load due to collector restrictions, resulting in the actual energy density of the battery is insufficient, and cannot meet the requirements of commercial applications [12]. In the last decade, natural binders have been favored by researchers because of their environmental friendliness, good mechanical and thermal stability, rich functional groups, and easy modification. researchers have developed a variety of natural binders, such as gum acacia [13], gelatin [14], sodium alginate [15], carrageenan [16]. Their good mechanical properties as well as abundant functional groups contribute to enhancing the sulfur cathode's performances significantly, which shows certain application potential. Therefore, there is an urgent need to develop an environmentally friendly, sustainable, aqueous and multifunctional sulfur cathode binder.

Ramie is a unique crop in China, mainly used for textiles. Generally speaking, the degumming step must be carried out in the process of ramie fiber processing. In this process, a large amount of degumming waste liquid will be produced and treated as domestic sewage [17]. Herein, we proposed RG as a sulfur cathode binder that is obtained by simulating the process of industrial ramie gum removal [18], and then by alcohol extraction and freeze-drying (Fig. 1a). Previous studies have shown that RG is mainly composed of low-esterified polygalacturonic acid (HG) and low-branched rhamnogalacturonic acid glycan I (RG-I), which provides abundant polar functional groups and a certain branching structure [19,20]. Additionally, it also includes a small number of nitrogen-containing substances, *i.e.*, proteins and nitrates [21]. Based on this, we believe that RG is a promising binder compared to the conventional binder for the sulfur cathode due to its excellent mechanical properties as well as strong anchoring effect on LiPSs (Fig. 1b). As expected, the pure sulfur cathode using RG as a binder shows excellent electrochemical performance. The reversible capacity of the sulfur cathode is as high as 644.6 mAh/g after 500 cycles under 0.5 C. Even under the high sulfur loading of 4.30 mg/cm^2, the area capacity of the corresponding sulfur cathode using RG could still maintain 3.1 mAh/cm^2 after 200 cycles.

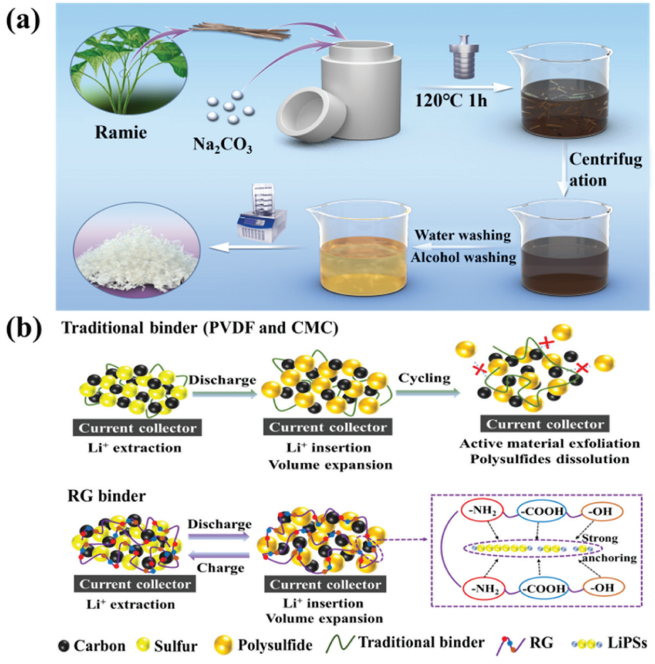

Fig. 1. (a) Schematic of the process of the preparation of RG. (b) The mechanisms of the impact of RG and conventional binder on sulfur cathode.

Firstly, the water solubility and the viscidity of RG have been tested. As shown in Fig. S1 (Supporting information), 0.45 g RG is easy to dissolve in 30 mL distilled water after stirring for 3 h, which has been verified its good solubility in water. And the resulting RG solution shows the rotary viscosity of 555.5 mPa s in Table S1 (Supporting information), which is higher than that of PVDF (20.4 mPa s) but a little lower than that of CMC (1023 mPa s). Low viscosity will make it difficult for the active material to adhere on the current collector, while too high viscosity will cause poor fluidity of the electrode slurry, resulting in uneven distribution of active substances [22], so the RG has a suitable viscosity to form the slurry, which gives the RG the prospect of practical application as electrode binder. Then the morphology and composition of the extracted RG binder were characterized. As shown in Fig. S2 (Supporting information), the RG shows a granular morphology, and its size is about 10–20 μm. Then, FT-IR was conducted. As shown in Fig. 2a, the RG shows peaks at 3540 and 3220 cm^{-1}, corresponding to the stretching vibration of O–H and N–H groups, respectively [23]. A peak at 2927 cm^{-1}, corresponds to the stretching vibrations of C–H bonds, and the peaks at 1606 and 1090 cm^{-1} are from O–C-O bonds' symmetric/asymmetric vibrations [24,25]. Additional weak absorption peaks appearing at the low-frequency range of 1014 cm^{-1} is ascribed to C–O vibrations [26,27]. Additionally, we also conducted the XPS characterization for RG, as shown in the full XPS spectra of RG in Fig. 2b, there are C, N, and O elements in RG binder. More importantly, the content of N and O elements are as high as 1.87 wt% and 41.7 wt%, respectively. The high-resolution XPS spectra of further N 1s in Fig. 2d shows that the N elements contained in the RG binder are pyrrole nitrogen, pyridine nitrogen and graphite nitrogen, among which pyrrole nitrogen is dominant and the previous research reported that the pyrrole nitrogen is most favorable to adsorb LiPSs [23,28], besides, it can also be observed the -OH (533 eV), -C=O (288.4 eV) and -C-O (286.5 eV) bonds from the high-resolution XPS spectra of C 1s and O 1s (Figs. 2c and e), which are beneficial to anchoring the LiPSs as well [24,29–31]. Finally, we performed a liquid chromatography-mass spectrometry (HPLC-MS) test on the configured RG. As shown in Fig. S3 (Supporting information), RG contains various sugar molecules including D-galacturonic acid, L-rhamnose, D-galactose, and lactose, which are in consistent with previous reports[19,20]. In addition, there are some other possible ingredients, including glutamic acid and alanine [21]. Fig. S4 (Supporting information) shows the corresponding structural formula of these main substances. Obviously, these substances are rich in carboxyl, amino and hydroxyl groups, which is consistent with the results of FT-IR and XPS characterization. Therefore, they all proved that RG is rich in oxygen-containing and nitrogen-containing functional groups, which is conducive to limiting the shuttle of LiPSs.

In order to verify the superiority of RG binder for Li-S batteries, we fabricated cells based on RG, CMC, and PVDF. Before testing the electrochemical performances of S@RG, the CV curve for RG cathode was tested at the voltage of 1.5–3.0 V. As can be seen in Fig. S5 (Supporting information), RG as the cathode has no obvious redox peak between 1.5 V and 3.0 V, indicating that it is electrochemically inactive during this voltage range. Figs. S6-S8 (Supporting information) illustrate the CV curves of S@RG, S@CMC and S@PVDF cathodes during the first 3 cycles. It can be observed two reduction peaks of S@RG cathode at 2.1 and 2.3 V, corresponding to the conversion of S_8 to higher-order Li_2S_n ($4 \le n \le 8$) and then to Li_2S_2/Li_2S, and an oxidation peak at 2.4 V, corresponding to oxidizing Li_2S to Li_2S_n ($4 \le n \le 8$). And it can be also observed that the S@RG cathode shows better overlap of the CV curves (Fig. S6 in Supporting information) during the first 3 cycles, indicating better reversibility of S@RG compared to S@CMC (Fig. S7 in Supporting information) and S@PVDF (Fig. S8 in Supporting information). More importantly, RG-based electrode presents smaller difference

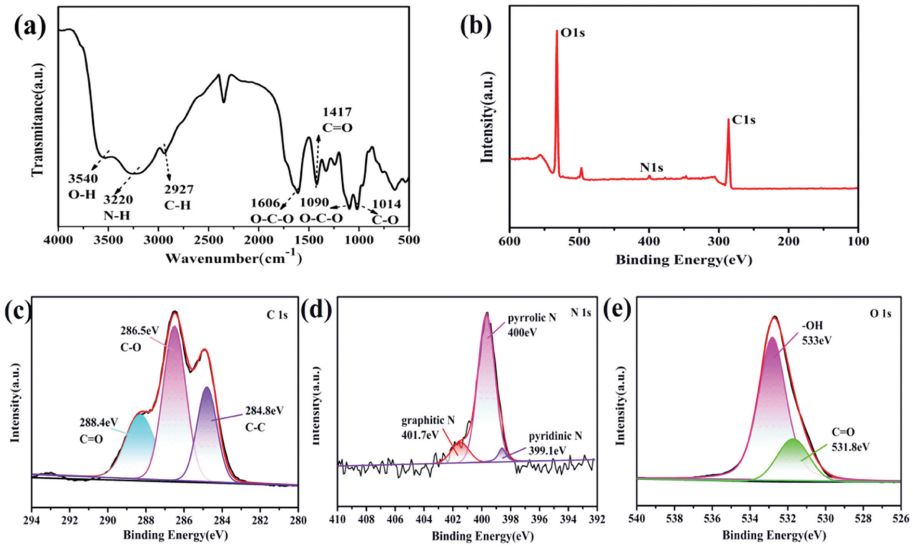

Fig. 2. Characterizations for the RG binders: (a) FTIR spectra of RG, (b) full XPS spectrum of RG. The high-resolution XPS spectra of (c) C 1s, (d) N 1s and (e) O 1s.

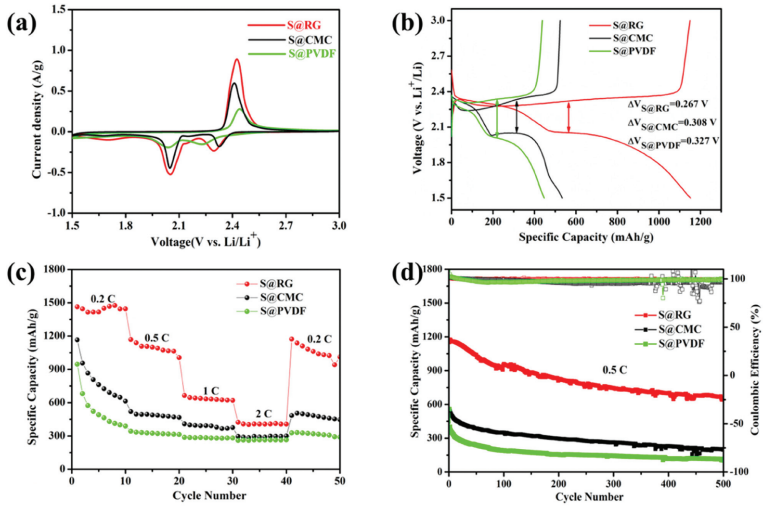

Fig. 3. Electrochemical performances comparison between S@RG, S@CMC and S@PVDF cathode: (a) The CV curves comparison of the first cycle between S@RG, S@CMC and S@PVDF. (b) The first cycle charge/discharge curves of S@RG, S@CMC and S@PVDF cathodes at 0.5 C. (c) The rate capability of S@RG, S@CMC and S@PVDF cathodes. (d) The long cycling performances comparison of S@RG, S@CMC and S@PVDF cathodes at 0.5 C after 3 cycles of activation at 0.1 C.

between oxidation and reduction peak potentials and higher peak currents (Fig. 3a), indicating that it has more rapid conversion kinetics than other two electrodes. Fig. 3b illustrates the charge-discharge profiles of S@RG, S@CMC and S@PVDF cathodes for the first cycle. There are two plateaus, consistent with the two reduction peaks in the CV curves. More importantly, it can be observed the voltage gap between the charge plateau and discharge plateau for S@RG is only 0.267 V, far smaller than that of S@PVDF (0.327 V) and S@CMC (0.308 V), which is proved the lower polarization of S@RG as well.

Figs. 3c and d compared the rate capability and cycling stability of S@RG, S@CMC and S@PVDF cathodes. Compared with CMC- and PVDF-based Li-S batteries, the RG-based Li-S battery show the maximum capacity at all tested C rates. Moreover, it is worth mentioning that the capacity of RG-based Li-S battery is 423.1 mAh/g at a high discharging rate of 2 C, while the CMC- and PVDF-based batteries show only 296.2 and 260.5 mAh/g at the same conditions, respectively. When the ampere density declines from 2 C to 0.2 C, the RG-based cell reversibly reverts to the capacity of 1172.3 mAh/g. Nevertheless, the CMC- and PVDF-based Li-S batteries show much lower reversible capacities (483.7 and 326.8 mAh/g) at 0.2 C. In the prolonged cycling test, the initial capacity of the Li-S battery fabricated with the RG binder is 1152.2 mAh/g at 0.5 C, and it remains 644.6 mAh/g with a capacity attenuation of only 0.087% per cycle after 500 cycles. On the contrary, Li-S batteries manufactured with CMC and PVDF binders show initial capacities of only 533.6 and 558.1 mAh/g at 0.5 C, respectively. Apparently, RG as a binder ensures the sulfur cathodes with excellent cycling stability, far better than conventional binder, and even outperforming many other natural polymers that have been reported as shown in Table S2 (Supporting information). For the purpose of achieving a high practical energy density, the increase of sulfur loading is essential [32]. Therefore, a high-loading battery was assembled and tested. Fig. S9 (Supporting information) shows the charge-discharge voltage platform under different cycles when the sulfur loading is 4.30 mg/cm^2, and shows the typical redox behaviour of Li-S batteries. With the increase of the number of cycles, the charge-discharge potential platform is basically unchanged, and the capacity decreases slightly, which indicates that the RG-based electrode exhibits excellent cycle stability even at high active ma-

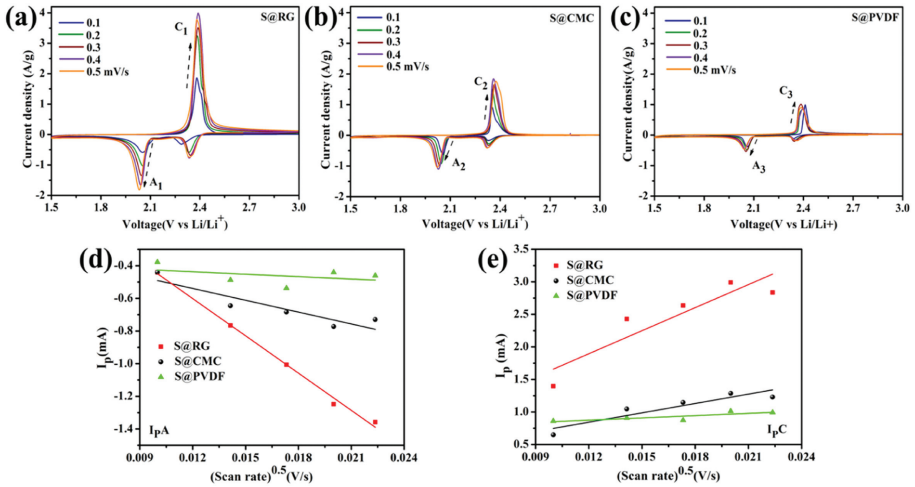

Fig. 4. The mechanism verification of sulfur electrode kinetic improvement by RG: CV curves of S cathodes by (a) RG, (b) CMC and (c) PVDF binders with scanning speeds from 0.1 mV/s to 0.5 mV/s. The linear fittings of (d) the cathode and (e) the anode peak currents *versus* $v^{0.5}$.

terials loading. The cycling performances under the high loading of 4.30 mg/cm^2 shows in Fig. S10 (Supporting information), which the discharge capacity could still maintain 3.1 mAh/cm^2 after 200 cycles. What is more, high Coulombic efficiency of 99.97% could achieve after 200 cycles, indicating that even under high sulfur loading, the RG binder can still effectively suppress the shuttle effect, and ensure the high surface capacity.

The above electrochemical performances demonstrate the superiorities of RG as a binder for the sulfur cathode, which can stabilize the electrode structure and restrain the shuttling effect in the Li-S batteries by anchoring LiPSs. In order to deeply understand the mechanisms, a series of characterizations have been conducted to explain. First the electrochemical characterizations verify the kinetic improvement of the electrode have been conducted. The CV curves of RG- (Fig. 4a), CMC- (Fig. 4b), and PVDF-based (Fig. 4c) sulfur cathodes at scanning speeds ranging from 0.1 mV/s to 0.5 mV/s were investigated. The Randles-Sevcik equation has been utilized to calculate the lithium-ion diffusion coefficient (D_{Li}) [33].

$$I_p = 2.69 \times 10^5 n^{1.5} A D_{Li}{}^{0.5} v^{0.5} C_{Li} \quad (1)$$

Here I_p is the peak current (A), v is the scan speed (V/s), n is the number of transfer electron during the reaction, A is the reaction area of the electrode (cm^2), D is the diffusion coefficient (cm^2/s), and C_{Li} is the concentration of lithium ion (mol/L).

The linear fittings are applied to a cathode peak current (Fig. 4d) and an anode peak current (Fig. 4e) *versus* the square root of the scanning speeds. The linear relationships between the peak current and the square root of the scanning speeds are in good agreement with the Randles-Sevcik equation. Moreover, it can be seen from the equation that the slope of the chart is positively related to the diffusion efficient (D_{Li}). The slopes of plots derived from the RG- and CMC-based electrodes are significantly larger than those of PVDF-based electrodes for the reason that lots of oxygen and nitrogen containing functional groups in the RG can achieve high Li^+ conduction by the hopping among coordination sites and the "locked" anions [34]. The calculated D_{Li} are listed in Table S3 (Supporting information). The results show that the D_{Li} of S@RG is much higher than those of S@CMC (10 times) and S@PVDF (100 times), proving that the RG significantly facilitates the transport of Li-ions.

We also conducted the EIS test of the sulfur cathode before and after cycling. Characteristic Nyquist plots in Fig. S11 (Supporting information) show an intercept at a high-frequency region (R_s, ohmic resistance), a semicircle at medium-frequency (R_{ct}, charge-transfer resistance), and an inclined line at low-frequency region (W_c, Warburg impedance) to the real axis [30]. As can be seen, before discharging, there is only one semicircle for all three sulfur cathodes, attributed to the R_{ct} at the interface between the electrolyte and sulfur cathode. Typically, all the electrodes exposed similar solution resistance as shown in Table S4 (Supporting information). However, the R_{ct} value of S@RG illustrated in Table S4 is only 67.89 Ω, whereas higher values were evident for S@CMC at 90.1 Ω and S@PVDF at 112.8 Ω, indicating feasible binder interface for active sulfur and Li-ion interaction to offer improved ionic and electronic conductivity in S@RG electrodes. After discharging 100 cycles (Fig. S12 in Supporting information), S@CMC and S@PVDF cathodes both illustrate two semicircles in high and medium frequency regions, respectively, corresponding to the solid-electrolyte-interface (SEI) film resistance and the interfacial charge transfer resistance that is caused by the formation of Li_2S/Li_2S_2. While the S@RG cathode still only illustrate a one semicircle in high frequency, which indicate that the LiPSs have been effectively inhibited, as a result the unwanted discharge products Li_2S/Li_2S_2 formed very few [35]. Additionally, after 100 cycles, the R_{ct} value of S@RG becomes smallest compared to that of S@CMC and S@PVDF (Table S4), which suggest the RG could be beneficial to enhancing the transportation of Li-ions during charge/discharge. Accordingly, both the CV and EIS characterizations have been verified the enhancement of the kinetic by employing the RG binder, which would remarkably enhance the rate capability and active substance utilization.

As is known, the strong affinity of the binder to polysulfides is an important factor that contributes to improving electrochemical performance. Thus, we then conducted polysulfides adsorption experiments to study the potential adsorption ability of various binders. The adsorption experiment of different binders soaking in Li_2S_4 solutions after 6 h has been tested. It can be seen in Fig. 5a that the RG binder has strong adsorption capability for Li_2S_4, and the color of the solution is almost transparent. This can be attributed to the excellent adsorption performance of the functional groups of RG. From the UV–vis spectra in Fig. 5b, it is found that the absorption peak of Li_2S_4 does not decrease obviously with the addition of CMC and PVDF binder. On the contrary, after adding RG binder, the absorption peak intensity of Li_2S_4 dramatically decreases, also indicating that RG plays a key adsorption role in the adsorption of Li_2S_4 [30]. Following the XPS characterization for

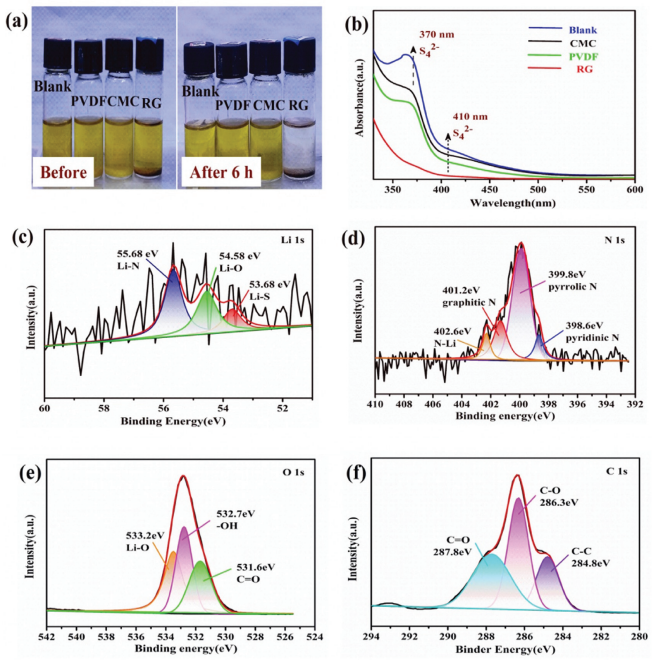

Fig. 5. Mechanism verification of RG binder anchoring LiPSs: (a) Photographs of LiPSs solution (Li_2S_4, 2 mmol/L) before and after 6 h treatment with different binders. (b) UV–vis spectra of the LiPSs solution treated by different binders. High-resolution XPS spectra of (c) Li 1s, (d) N 1s, (e) O 1s and (f) C 1s of RG after LiPSs immersion.

the RG after soaking in Li_2S_4 solution is conducted as well. It can be observed the peaks of C, O, N, S, and Li elements in the full XPS spectrum (Fig. S13 in Supporting information). More importantly, it can be observed the peaks of Li-N bond at 402.6 eV and 55.68 eV from the high resolution of N 1s (Fig. 5c) and Li 1s spectrum (Fig. 5d) [25], respectively. Simultaneously, the -OH (533 eV), -C=O (513.8 eV) and -C-O (286.5 eV) bonds in Figs. 5e and f shift downward to 532.7, 531.6 and 286.3 eV compared to that in Figs. 2c and e, respectively. All the changes in chemical bonds indicate the strong chemical adsorption of RG on LiPSs, which are beneficial for inhibiting the LiPSs shutting and improving the cycling stability and rate capability.

Thirdly, the mechanical property of the binder also plays an important role in the electrochemical performance of Li-S batteries, which can withstand the volume change of the sulfur cathode and maintain electrode integrity during cycling. The adhesion strength of different adhesives RG, CMC and PVDF was compared by peeling force test at 180°. As shown in Fig. 6a, the bonding strength of the RG binder (2.43 N) is higher than that of CMC (1.84 N) and PVDF (1.81 N), which indicates that the RG has stronger mechanical properties and can closely connect the active material and the conductive agent to maintain the integrity of the electrode structure [26]. For the nanoindentation experiments, it can be observed that under the same load, the indentation depth on the S cathode using RG binder is higher than that on the sulfur cathode using CMC and PVDF binder (Fig. 6b), so the S cathode using the RG binder has better flexibility. Moreover, from Fig. 6c, it can be observed that the average elastic modulus of S@RG cathode is 1.64 GPa, while the average elastic modulus of the S@CMC and S@PVDF adhesives is 3.14 and 0.59 GPa. And from Fig. 6c, it can be observed that the hardness of S@RG cathode is 0.045 GPa, while the hardness of the S@CMC and S@PVDF adhesives are 0.011 and 0.035 GPa, respectively. These suggest the elasticity and hardness of RG are weaker than CMC but stronger than PVDF. As is known, binder with strong hardness but low elasticity is more susceptible to fracture under a critical stress, especially for high mass loading active materials. While if a binder with only strong elasticity but weak hardness, it cannot address the problems of electrode swelling [27,36,37]. Therefore, a superior binder should possess appropriate hardness and elasticity simultaneously. Luckily, the RG binder owns both, which enables to delay the collapse caused by the change in the volume of the active material and maintains the structural integrity of the electrode during charging/discharging. Thus, the cycle stability of the electrode is effectively improved.

To visually observe the effect of RG binder on the mechanical stability of sulfur cathode, SEM images of the sulfur cathode before and after cycling were conducted too. Figs. 6d-i compare the morphology of sulfur cathodes with RG, CMC and PVDF binders before and after 100 cycles. SEM observation confirmed that the electrode morphology of S@RG, S@CMC and S@PVDF was significantly different. Before cycling, small cracks (Figs. 6e and f) appeared in the CMC- and PVDF-based cathodes due to weaker mechanical and adhersion propterties. On the contrary, the active materials and conductive agents were firmly adhered to the current collector (Fig. 6d) due to the appropriate viscosity of RG. After cycling 100 cycles, due to the continuous expansion and contraction during the cycling process, large cracks and large aggregations appear in the S@CMC (Fig. 6h) and S@PVDF (Fig. 6i) cathodes, which will lead to serious loss of active materials and capacity attenuation. However, the RG-based (Fig. 6g) sulfur cathode maintains a perfect surface morphology and does not crack after 100 cycles due to excellent adhesion and mechanical properties, which ensures high lithium-ion diffusion and close contact between the sulfur composite and the conductive agents. The better surface morphology also leads to fast kinetic reactions, good electrical conductivity and enhanced cycle stability [38].

In addition to the characterization of the positive sulfur electrode, we also characterized the lithium anode before and after cycling. As shown in Fig. S14a (Supporting information), before cycling, the surface of the lithium anode is smooth and flat. After discharging 100 cycles, as shown in Figs. S14b and c (Supporting information), there are large amount of lithium dendrites growth on the surface of lithium anode in PVDF and CMC-based cells, and the lithium anodes surface corrosion is serious. However, the surface corrosion of the lithium anode in the RG-based cells is less obvious (Fig. S14d in Supporting information), and the growth of lithium dendrites is also less. This also shows that the use of RG binder reduces the shuttle of LiPSs to the lithium anode, resulting in dendrite growth and surface corrosion.

According to the above series of characterization verification, the mechanisms of RG on improving the electrochemical performances of S cathode in Fig. 1b have been verified, that is, RG is a high molecular compound extracted from natural plants, it has a strong and flexible structure as well as good mechanical properties, which can limit the volume expansion of active substances during charging and discharging and inhibit the cracking of electrodes. In addition, the strong electronegativity generated by the nitrogen-containing functional groups and oxygen-containing functional groups on the RG skeleton is easy to capture LiPSs through the secondary valence bond force [24]. Therefore, the shuttle effect was alleviated and the adverse reactions caused by LiPSs diffusion were also inhibited. As a sharp contrast, traditional binders have struggled to maintain the integrity of cathode and repress the shuttle effect.

In summary, the feasibility of extracting ramie gum from ramie fiber degumming liquid as positive electrode binder for Li-S battery was investigated. The experimental results show that the ramie gum has comparable adhesion strength to the commercial PVDF and CMC binders, and better mechanical properties and fixing ability of LiPSs. With employing the ramie binder, the sulfur cathode could reach a superior high specific discharge capacity of 1152.2

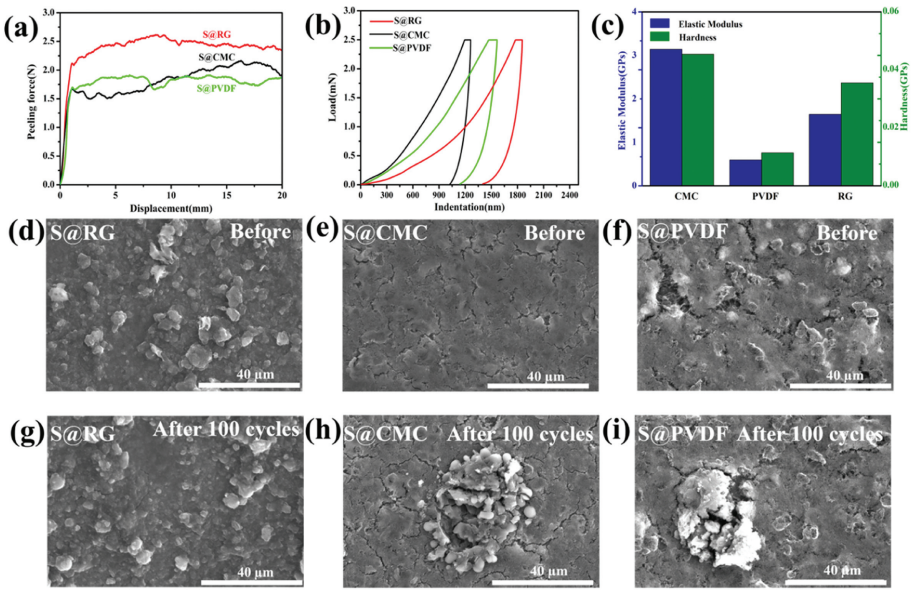

Fig. 6. Mechanism verification of improving mechanical properties of RG binder: (a) Peel strength of the S@RG, S@CMC, and S@PVDF electrodes. (b) Typical load-indentation depth curves of the S@RG, S@CMC, and S@PVDF electrodes. (c) Elastic modulus and Hardness of S cathodes using RG, PVDF, and CMC binders. (d-f) SEM images of S@RG, S@CMC and S@PVDF cathodes before 100 cycles. (g-i) SEM images of S@RG, S@CMC and S@PVDF cathodes after 100 cycles.

mAh/g at 0.5 C and maintain a reversible discharge capacity of 644.6 mAh/g after 500 cycles. The capacity decay rate was only 0.087% per cycle, which was far better than that of the sulfur cathode using CMC and PVDF binders. The results show that RG is a kind of high-performance sulfur cathode binder with potential application value, and simultaneously, the utilization of RG in battery binders also provides a new available strategy for recycling industry biomass.

Declaration of competing interest

The authors declare that they have no known competing financial interests or personal relationships that could have appeared to influence the work reported in this paper.

Acknowledgments

This work was supported by the National Natural Science Foundation of China (Nos. 51902036, 52071295, 52002352), Natural Science Foundation of Chongqing Science & Technology Commission (Nos. cstc2019jcyj-msxm1407 and CSTB2022NSCQ-MSX0828), the Venture & Innovation Support Program for Chongqing Overseas Returnees (No. CX2021046), the Science and Technology Research Program of Chongqing Municipal Education Commission(No. KJZD-K202300802) and Research Project of Innovative Talent Training Engineering Program of Chongqing Primary and Secondary School (No. CY230801).

Supplementary materials

Supplementary material associated with this article can be found, in the online version, at doi:10.1016/j.cclet.2024.109853.

References

[1] Z. Zhu, T. Jiang, M. Ali, et al., Chem. Rev. 122 (2022) 16610–16751.
[2] Q. Xiao, J. Yang, X. Wang, et al., Carbon Energy 3 (2021) 271–302.
[3] S. Ma, Q.L. Ruan, X.C. Liu, et al., Tungsten 6 (2024) 504–521.
[4] X.X. Gu, Z.G. Yang, S. Qiao, et al., Rare Metals 40 (2021) 529–536.
[5] Y. Zhao, Z. Gu, W. Weng, et al., Chin. Chem. Lett. 34 (2023) 107232.
[6] J. Zhang, M. Li, H.A. Younus, et al., Nano Mater. Sci. 3 (2021) 124–139.
[7] X.B. Cheng, S.J. Yang, Z. Liu, et al., Adv. Mater. 36 (2024) 2307370.
[8] Y. Li, G. Zhang, B. Chen, et al., Chin.e Chem. Lett. 33 (2022) 3287–3290.
[9] S.J. Yang, N. Yao, F.N. Jiang, et al., Angew. Chem. Int. Ed. 61 (2022) e202214545.
[10] W. Dou, M. Zheng, W. Zhang, et al., Adv. Funct. Mater. 33 (2023) 2305161.
[11] Z. Li, Y. Zhang, T. Liu, et al., Adv. Energy Mater. 10 (2020) 1903110.
[12] Z. Lin, C. Liang, J. Mater. Chem. A 3 (2015) 936–958.
[13] G. Li, M. Ling, Y. Ye, et al., Adv. Energy Mater. 5 (2015) 1500878.
[14] Y. Wang, Y. Huang, W. Wang, et al., Electrochim. Acta 54 (2009) 4062–4066.
[15] X. Hong, J. Jin, Z. Wen, et al., J. Power Sources 324 (2016) 455–461.
[16] G. Ai, Y. Dai, Y. Ye, et al., Nano Energy 16 (2015) 28–37.
[17] J. Neto, H. Queiroz, R. Aguiar, et al., J. Renew. Mater. 10 (2022) 561.
[18] F. Brühlmann, M. Leupin, K.H. Erismann, et al., J. Biotechnol. 76 (2000) 43–50.
[19] J. Wang, Z. Liu, X. Li, et al., Carbohyd. Polym. 314 (2023) 120954.
[20] W. Jiang, Y. Song, S. Liu, et al., Ind. Crop. Product. 120 (2018) 131–134.
[21] M. Rehman, D. Gang, Q. Liu, et al., Ind. Crop. Product. 137 (2019) 300–307.
[22] L. Cheng, Y. Sun, C. Ma, et al., Chem. Engin. J. 431 (2022) 133703.
[23] X.X. Gu, Z.G. Yang, S. Qiao, et al., Rare Metals 40 (2020) 529–536.
[24] C. Li, Q. Sun, Q. Zhang, et al., Chem. Engin. J. 455 (2023) 140706.
[25] Z. Huang, L. Wang, Y. Xu, et al., Chem. Engin. J. 443 (2022) 136347.
[26] H. Wang, Y. Wang, P. Zheng, et al., ACS Sustain. Chem. Engin. 8 (2020) 12799–12808.
[27] T. Liu, Q. Chu, C. Yan, et al., Adv. Energy Mater. 9 (2019) 1802645.
[28] X. Chen, G. Du, M. Zhang, et al., J. Electroanal. Chem. 848 (2019) 113316.
[29] Y. Yang, J. Qiu, L. Cai, et al., ACS Appl. Mater. Interfaces 13 (2021) 33066–33074.
[30] C. Senthil, S.S. Kim, H.Y. Jung, Nat. Commun. 13 (2022) 145.
[31] W. Chen, T. Lei, T. Qian, et al., Adv. Energy Mater. 8 (2018) 02889.
[32] H. Yu, M. Bi, C. Zhang, et al., Electrochim. Acta. 428 (2022) 140908.
[33] W. Zeng, L. Wang, X. Peng, et al., Adv. Energy Mater. 8 (2018) 1702314.
[34] X. Fu, L. Scudiero, W.H. Zhong, J. Mater. Chem. A 7 (2019) 1835–1848.
[35] J.J. Yuan, Q.R. Kong, Z. Huang, et al., J. Mater. Chem. A 9 (2021) 2970–2979.
[36] S. Choi, T.W. Kwon, A. Coskun, et al., Science 357 (2017) 279–283.
[37] H. Wang, P. Zheng, H. Yi, et al., Macromolecules 53 (2020) 8539–8547.
[38] W. Bao, Z. Zhang, Y. Gan, et al., J. Energy Chem. 22 (2013) 790–794.